Structure and magnetic properties of Os_n ($n = 11 \sim 22$) clusters*

Zhang Xiu-Rong(张秀荣)[a)†], Zhang Fu-Xing(张福星)[b)], Chen Chen(陈 晨)[b)], and Yuan Ai-Hua(袁爱华)[c)]

[a)] School of Mathematics and Physics, Jiangsu University of Science and Technology, Zhenjiang 212003, China
[b)] School of Materials Science and Engineering, Jiangsu University of Science and Technology, Zhenjiang 212003, China
[c)] School of Biology and Chemical Engineering, Jiangsu University of Science and Technology; Zhenjiang 212003, China

(Received 9 March 2013; revised manuscript received 25 April 2013)

The structure and magnetic properties of Os_n ($n = 11 \sim 22$) clusters are systematically studied by using density functional theory (DFT). For each size, the average binding energy per atom, the second-order differences of total energies and the highest occupied molecular orbital (HOMO)– the lowest unoccupied molecular orbital (LUMO) gaps are calculated to analyze the stability of the cluster. The structures of Os_{14} and Os_{18} clusters are based on a close-packed hexagonal structure, and they have maximum stabilities, so $n = 14$, 18 are the magic numbers. The 5d electrons play a dominant role in the chemical reaction of Os_n clusters. The magnetic moments of Os_n clusters are quenched around $n = 12$, and when $n = 18 \sim 22$ the value approximates to zero, due to the difference of electron transfer.

Keywords: density functional theory, Os_n clusters, structure, magnetic properties

PACS: 31.15.E–, 36.40.Cg, 36.20.Hb, 36.40.–c **DOI:** 10.1088/1674-1056/22/12/123102

1. Introduction

The cluster plays its role the same as a bridge linking molecule and bulk. The electronic structures and magnetic properties of clusters are very important parts in academic research. Among them, the transition metal (TM) clusters have been of special interest both theoretically and experimentally because of their potential as catalysts and high-density magnetic data storage materials.[1–10] However, compared with the clusters with 3d or 4d electrons, TM clusters with 5d electrons have been theoretically studied very little. Osmium as a member of the 5d electron elements is one of the most important parts of organic catalytic activity, but the investigations of its relevant clusters and complexes are few and far between.

In previous investigations, the hardness of osmium complexes and the catalytic activity of osmium carbonyls are the most popular projects. Ahrens *et al.*[11] studied the reactions of $[Os_3(CO)_{10}(MeCN)_2]$ with ethynyl thiophenes. The result indicates that the highest occupied molecular orbital (HOMO)–the lowest unoccupied molecular orbital (LUMO) gap decreases only marginally and suggests that the degree of conjugation in the cluster complexes is not much greater than that in the free ligands. Jackson and Walls[12] studied the catalysis of osmium metal clusters by using a combination of analytical techniques; an overall picture and the chemisorption and catalytic studies all show behavior fundamentally different from that obtained with conventional metal catalysts. Zhang *et al.*[13] studied the chemical bondings, elastic behaviors, phase stabilities, and hardness values of OsB, OsB_2, OsC, OsO_2, OsN, and OsN_2 by using first-principles calculations. The calculations suggest that the chemical bondings in these compounds are a mixture of covalent and ionic components. The results indicate that the hexagonal tungsten carbide structure is more stable, the large occupations and high strength of the covalent bonds are crucial for a superhard material, and there is no clear connection between bulk modulus and hardness in these osmium compounds. Yang *et al.*[14] investigated the structure in the frame of the generalized gradient approximation (GGA) and (local density approximation (LDA) by using CASTEP code, elastic properties, and elastic anisotropy of orthorhombic OsB_2 under pressure. They found that the elastic constants, bulk modulus, and Debye temperature of OsB_2 tend to increase with pressure increasing. It is predicted that OsB_2 is not a superhard material. Ji *et al.*[15] studied the mechanical properties and chemical bonding of the Os–B system, and the results indicate that high hardness values in Os_2B_5 and OsB_3 are mainly attributed to the occurrence of strong B–B covalent bonds and the disappearance of some ductile Os–Os metallic bonds.

Our research group[16–19] also studied the Os–N, Os–B cluster system and pure osmium clusters with small sizes ($n = 2 \sim 10$), but there have been hardly any other studies of pure osmium clusters so far, so we will continue this research. In this paper, we pay attention to structures, relative stabilities, and magnetic properties of Os_n clusters with $11 \leq n \leq 22$ by using density functional theory (DFT), so as to make a research foundation of the osmium application.

2. Theoretical methods

The structures and magnetic properties of Os_n ($n = 11 \sim 22$) clusters are computed using DFT semi-core pseudopots

*Project supported by the National Natural Science Foundation of China (Grant No. 51072072).
†Corresponding author. E-mail: zh4403701@126.com

in the DMOL3 package. In the calculation of the electronic structure, we use the spin-polarized generalized gradient approximation (GGA) with PW91 functional for the exchange–correlation interaction and the double numerical basis set that includes d-polarization functions (DND). The direct inversion in an iterative subspace (DIIS) approach is designed for speeding up the self-consistent field (SCF) convergence, and in the structure optimization we consider the smearing. The SCF calculation is done with a convergence criterion of 10^{-5} Hartree (1 Hartree = 2 Ry = 27.2114 eV). The density mixing criteria for charge and spin are taken to be 0.2 and 0.5 respectively. The smearing of molecular orbital occupation is 0.002 Hartree. In the geometry optimization, convergence thresholds are set to be 0.004 Hartree/Å for the forces, 0.005 Å for the displacement and 10^{-5} Hartree for the energy change. We design different initial configurations. Starting with the lowest spin multiplicity for Os_n cluster, spin-unrestricted calculations are performed to find the low-lying metastable isomers whose frequency is positive, and then some relative properties of ground-state structure are calculated.

To verify the effectiveness of the proposed method, we calculate the dimer Os_2 and find the bond length to be 2.215 nm, which is very close to the experimental value (2.28 nm).[20]

3. Results and discussion

3.1. Geometrical structure

Figure 1 gives the ground-state structures and some low-lying metastable isomers obtained for Os_n ($n = 11 \sim 16$) clusters in this work. The spin multiplicity, symmetry and the relative energy of each structural isomer from the ground state are also labeled below the corresponding structural plot of Fig. 1.

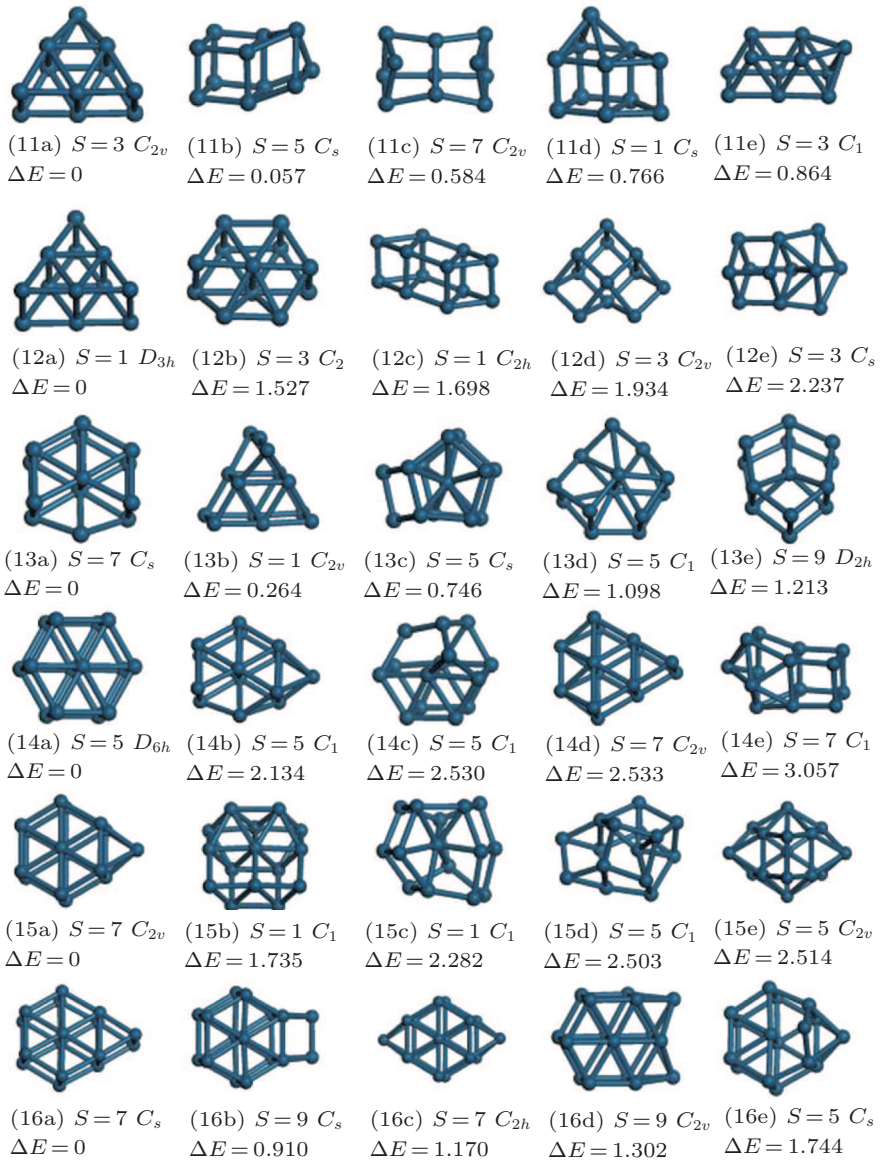

Fig. 1. (color online) Stable structures of Os_n ($n = 11 \sim 16$) clusters.

Lots of stable structures are obtained in geometry optimization, so we pick out five of the most stable structures in Fig. 1. In the isomers of Os_{11} cluster, pyramid geometry with C_{2v} symmetry (11a) has the lowest energy. The structure combined with cube and triangle with C_s symmetry (11b) lies only 0.057 eV higher than the ground-state structure in total energy. The remaining three structures are very close to the ground-state structure in total energy. The ground-state structure of Os_{12} favors a trigonal prism with D_{3h} symmetry. The second stable structure is 1.527 eV higher than the ground-state structure in total energy which is very unstable compared with the lowest-energy structure, so is the third stable isomer. The ground-state structures of Os_n ($n = 13 \sim 18$) clusters are similar, because they are all based on the regular hexagonal prism which is the most stable structure of the Os_{14} cluster. In Os_{13} cluster, the most stable structure is the regular hexagonal prism losing one corner (13a) with the C_s symmetry. Adding one atom in the trigonal prism (12a), we obtain a structure (13b) with C_{2v} symmetry which is the second stable structure of Os_{13} cluster. The lowest-energy configuration of Os_{14} cluster is the regular hexagonal prism with two atoms on both undersurfaces, which has D_{6h} symmetry. In total energy, the ground-state structure of Os_{14} cluster is much lower than the second stable configuration (14b) which is added by one atom in the side face of the ground-state of Os_{13} cluster with C_1 symmetry ($E = 2.134$). In Fig. 1, there are also two structures without symmetry, which are irregular. The ground-state structure of Os_{15} cluster is face-capped hexagonal prism geometry with C_{2v} symmetry (15a). The cage-like geometry with C_s symmetry has a high relative energy of $E = 1.735$, and is the second biggest in total energy. The lowest-energy configuration of Os_{16} cluster can be obtained by adding two atoms on the same side face of the ground-state structure of Os_{14} cluster (14a) that has C_s symmetry. In Fig. 1, the remaining four isomers are also based on the (14a), and their relative energies are $\Delta E = 0.910$, $\Delta E = 1.170$, $\Delta E = 1.302$, and $\Delta E = 1.744$, respectively.

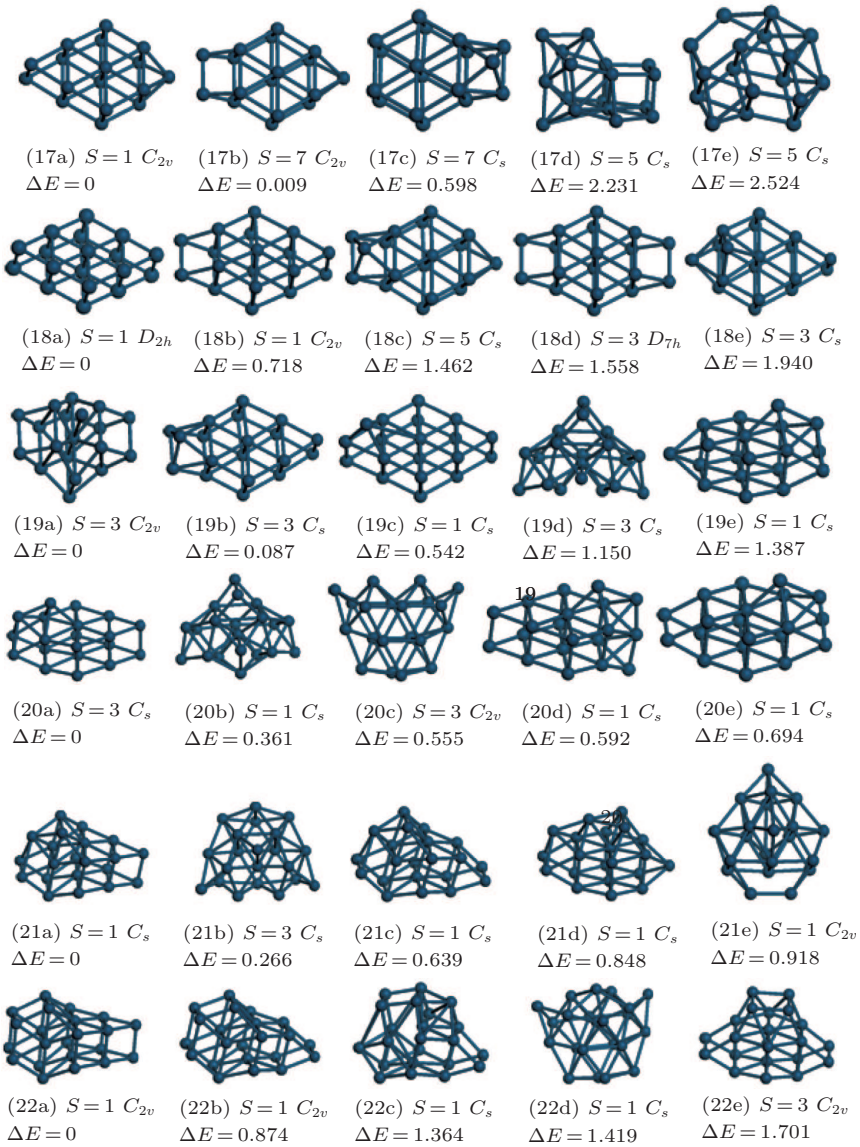

Fig. 2. (color online) Stable structures of Os_n ($n = 17 \sim 22$) clusters.

The low-lying geometries and lowest-energy structures of Os_n clusters with sizes from 17 to 22 are displayed in Fig. 2. Adding one atom on the opposite of the ground-state structure of Os_{16} cluster (16a) we can obtain the lowest-energy structure of Os_{17} cluster. Also, when we add one atom on the opposite of the second stable structure of Os_{16} cluster, we obtain the second stable structure of Os_{17} cluster, which is only 0.009 eV higher than the ground-state structure in total energy. For Os_{18} cluster, the quadrangle with undersurface of a rhombus (18a) is found to be the most stable structure, and has D_{2h} symmetry. Relative to the ground state, figure (18d) is a little different in configuration. The four atoms on both sides are arranged in the direction parallel to the undersurface, but the relative energy is much higher ($\Delta E = 1.558$). The second stable structure (18b) is a mixed structure of Figs. (18a) and (18d), its energy is also between those of the two configurations and it has C_{2v} symmetry. Adding one atom on the center of the (18d) structure, and then folding, there occurs the lowest-energy structure of Os_{19} cluster. The second and the third stable structure can be obtained by adding an atom on the (18b) and (18a) structures, and their relative energies are $\Delta E = 0.087$ and $\Delta E = 0.542$, respectively. From Os_{11} to Os_{18} cluster, their structures each turn into a cage that is somewhat compressed, but from Os_{19} to Os_{22} cluster, the configurations each seem to favor the globular cage although these cages are still based on the hexagonal prism. This means that with the increase of size, the structure and stability of the clusters change somewhat, and the transition starts from Os_{19} cluster.

3.2. Relative stability

For insight into the relative stabilities, the size-dependent physical properties are discussed in the following. The average binding energies per atom (E_b/atom) and the second-order differences of total energies ($\Delta_2 E$) are plotted in Figs. 3 and 4, respectively. The quantities of E_b and $\Delta_2 E$ are estimated in the following ways:

$$E_b(\mathrm{Os}_n) = nE(\mathrm{Os}) - E(\mathrm{Os}_n), \quad (1)$$

$$\Delta_2 E(\mathrm{Os}_n) = E(\mathrm{Os}_{n+1}) + E(\mathrm{Os}_{n-1}) - 2E(\mathrm{Os}_n), \quad (2)$$

where $E(\mathrm{Os}_n)$ is the total energy of the Os_n clusters, and $E_b(\mathrm{Os}_n)$ is the binding energy of the system.

As shown in Fig. 3, the variation trend of the average binding energies of osmium clusters can be divided into two phases. From the average binding energy curve of Os_{11} to Os_{19} clusters, there exhibits the odd–even oscillation effect, and from Os_{20} to Os_{22} clusters, the binding energy increases with cluster size increasing generally. For $n = 12$, 14, 16, 18, the stabilities of Os_n clusters are higher than those of their adjacent clusters. We plot the values of $\Delta_2 E$ as a function of cluster size in Fig. 4. From this figure, odd–even oscillation effect also occurs in the same range size. Four prominent peaks are found to correspond to $n = 12$, 14, 16, and 18, indicating that the clusters (especially for Os_{14} and Os_{18} clusters) possess the stronger stabilities than their neighbors, which is consistent with the trend of binding energies as shown in Fig. 3.

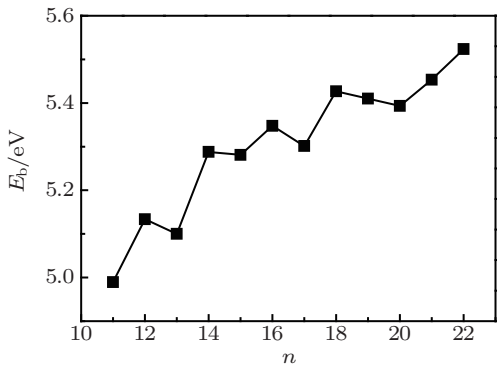

Fig. 3. Variation of average binding energy (E_b/atom) of osmium cluster with cluster size.

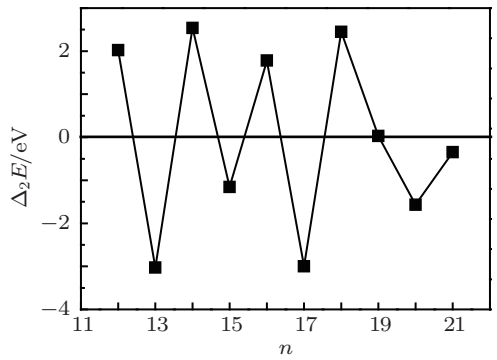

Fig. 4. Variation of the second-order difference of Os_n cluster energy ($\Delta_2 E(n)$) for the lowest-energy structure with cluster size n.

For the clusters ($n = 11 \sim 19$), even n gives high stability while odd n gives low stability. But from $n \geq 20$, the average binding energy of Os_n cluster increases monotonically with the increase of cluster size. This indicates that $n = 19$ is the turning point of the binding energy variation trend.

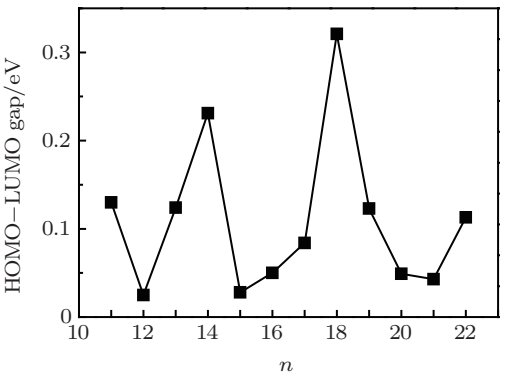

Fig. 5. Size-dependence of HOMO–LUMO gap of Os_n cluster for the lowest-energy structure.

The energy gap between HOMO and LUMO, which is $E_{gap} = E_{LUMO} - E_{HOMO}$, is generally considered as an important quantity to evaluate the stability of the cluster. The E_{gap} indicates the ability for an electron to transit from HOMO to LUMO. The smaller the value, the more easily the electron will transfer, and a larger E_{gap} signifies a weaker chemical activity and a higher stability of cluster. The HOMO–LUMO gaps of the ground-state structures of osmium clusters are plotted in Fig. 5. From this figure, one can easily see two prominent peaks at $n = 14$, 18, which suggest the tremendous stabilities of Os_{14} and Os_{18} clusters, and accord with the conclusions that are drawn from E_b and $\Delta_2 E$. This means that osmium clusters possess magic numbers of $n = 14$, 18. The structures of Os_{14} and Os_{18} clusters are based on close-packed hexagonal structure, as we know that the crystal lattice of osmium is a hexagonal dense lattice, which indicates that the consistency between theory and practice holds true only under certain conditions.

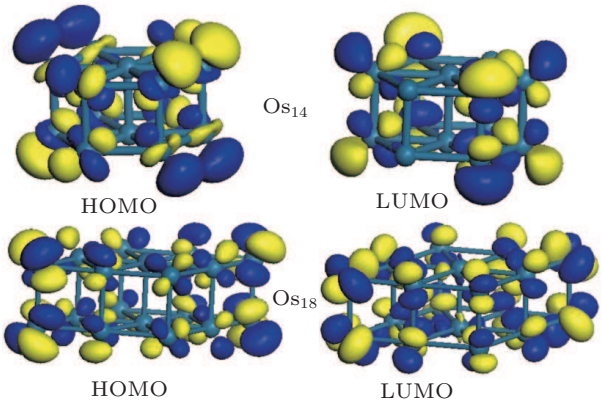

Fig. 6. (color online) Corresponding HOMO and LUMO orbital isosurfaces of Os_{14} and Os_{18} clusters.

The corresponding HOMO and LUMO orbital isosurfaces of these clusters are depicted in Fig. 6. Here we only take Os_{14} and Os_{18} clusters for example (because they are thought to be the most stable clusters in this article). Both HOMO and LUMO states are mainly located around the peripheral atoms of the clusters. It is seen clearly that HOMO and LUMO orbitals are completely contributed to by the 5d atomic orbitals. This indicates that 5d electrons play a dominant role in the chemical activities of osmium clusters.

3.3. Electronic and magnetic properties

To explore the size evolution of electronic properties, we analyze the partial densities of states (PDOSs) and total densities of states (TDOSs) for the lowest-energy Os_n clusters with sizes of $n = 11 \sim 22$ (provided in Figs. 7–9).

The Fermi level is presented as a vertical line and shifted to zero. Spin-α (up) and spin-β (down) densities are given in each figure (Figs. 7–9). As shown in most of the DOS figures, the d-orbit curve of PDOS is very similar to the curve of TDOS which is different from the s- and p-orbit curves, and the symmetry of d-orbit curve (except Os_{12} cluster) is lower, which indicates that there is a greater difference between the spin-up electronic number and the spin-down number, so all the electronic states come mainly from the 5d states compared with other states in Os atoms which are corresponding to the orbital analysis as mentioned before. In all the clusters, each d curve has a great spike, which indicates that the d electron exhibits locality compared with s and p curves. When $n = 11$, $13 \sim 16$, 19, 20, the symmetry of the DOS curve is much lower. This illustrates that there are many unpaired electrons around the atom. None of their spin multiplicities is 1, which also proves that the unpaired electrons are not very few. The other clusters have very high symmetry, of which the spin multiplicities are all 1. In the total DOSs from Os_{11} to Os_{18} cluster, there exist obvious local peaks near the Fermi level, but in the total DOSs from Os_{19} to Os_{22} cluster, the number of peaks reduces, and the local peak is less obvious than before, which is mainly because of the structural difference between clusters and accords with the stability analyzed before. Os_{12} cluster is an exception, the figure has horizontal symmetry, which may contribute to the magnetic moment quenching. The distance between two peaks which stay on each side of the Fermi level is defined as the pseudogap. The pseudogap can directly convey the strength of the covalent properties. The bigger pesudogap they have, the stronger covalent properties there will be. We can find that the pesudogaps of Os_{12}, Os_{14}, and Os_{18} clusters are bigger than those of the other clusters in Figs. 7–9, which indicates that those clusters have strong covalent bonds and stabilities, which is consistent with the previous analyses.

Based on the optimized geometries, the magnetic properties of Os_n clusters are computed. The total and the average magnetic moments are presented in Fig. 9. The total magnetic moments of Os_{13}, Os_{15}, and Os_{16} clusters are bigger than the others'. The average magnetic moment of Os_{11} cluster is 0.18 μ_B, and the average magnetic moment of Os_{12} cluster is zero, which is called "magnetic moment quenching". The atomic magnetic mainly comes from the spin of the electron and the movement of the orbital. When it occurs, the "magnetic moment quenches", and the electron magnetic moment changes its direction and cannot combine with the orbital magnetic moment, so there cannot be a resultant magnetic moment. Also, like the total magnetic moment, the average magnetic moments of Os_{13}, Os_{15}, and Os_{16} clusters are bigger than the others'. From Os_{18} to Os_{22} cluster, the average magnetic moments are very small, most of them are smaller than 0.1 μ_B, so indeed they can be said to be nonmagnetic approximately. For Os_{14} and Os_{18} clusters, they are highly symmetric but their magnetism is not so big. This may be caused by the difference in electron transfer, i.e., by adding an atom into or replacing an atom from a different place for a different structure: the difference in electron transfer may be great.

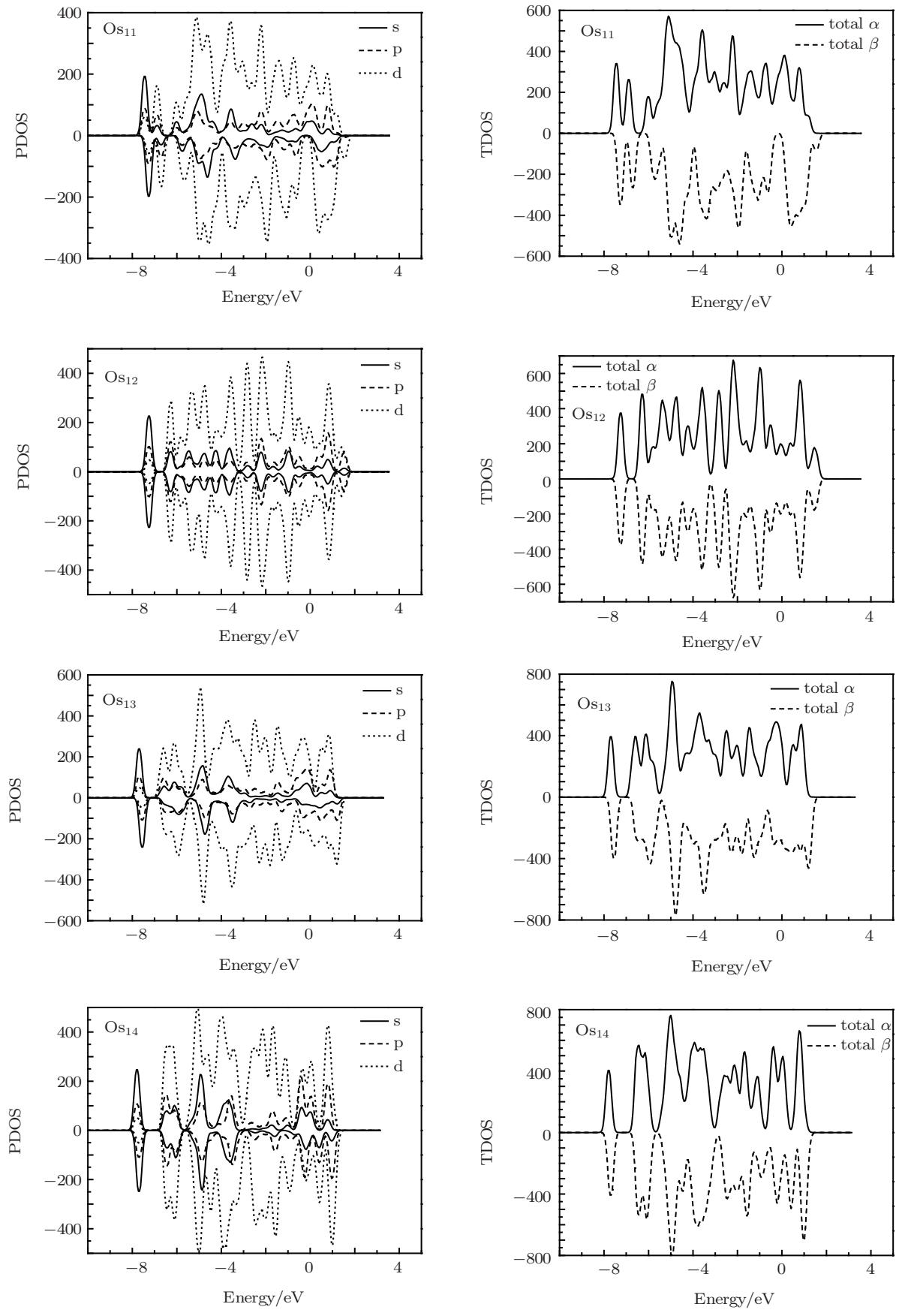

Fig. 7. Partial densities of states (PDOSs) of s, p, and d orbitals and total densities of states (TDOSs) of osmium clusters with $n = 11 \sim 14$. The vertical line indicates the Fermi level.

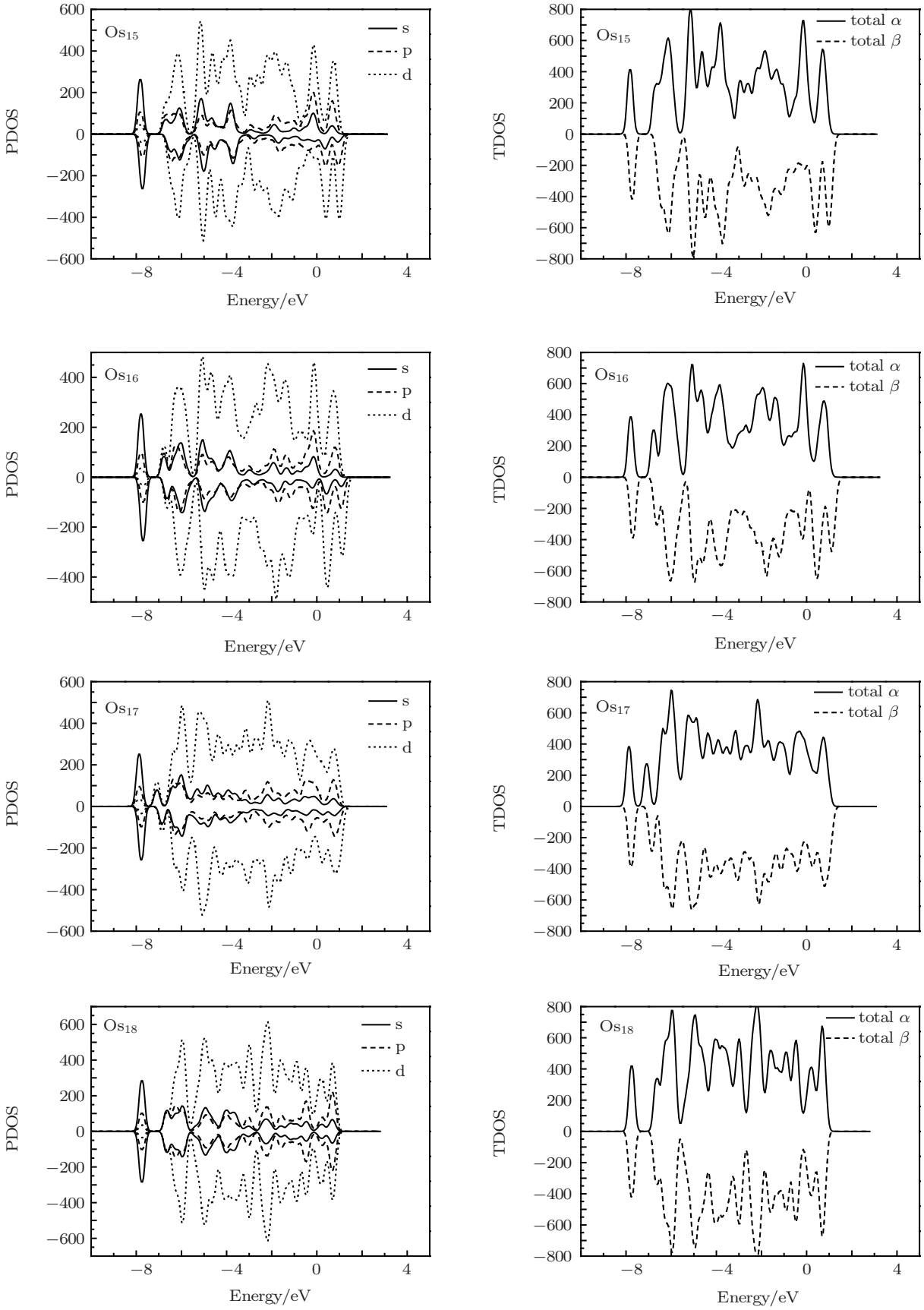

Fig. 8. Partial densities of states (PDOSs) of s, p, and d orbitals and total densities of states (TDOSs) of osmium clusters with $n = 15 \sim 18$. The vertical line indicates the Fermi level.

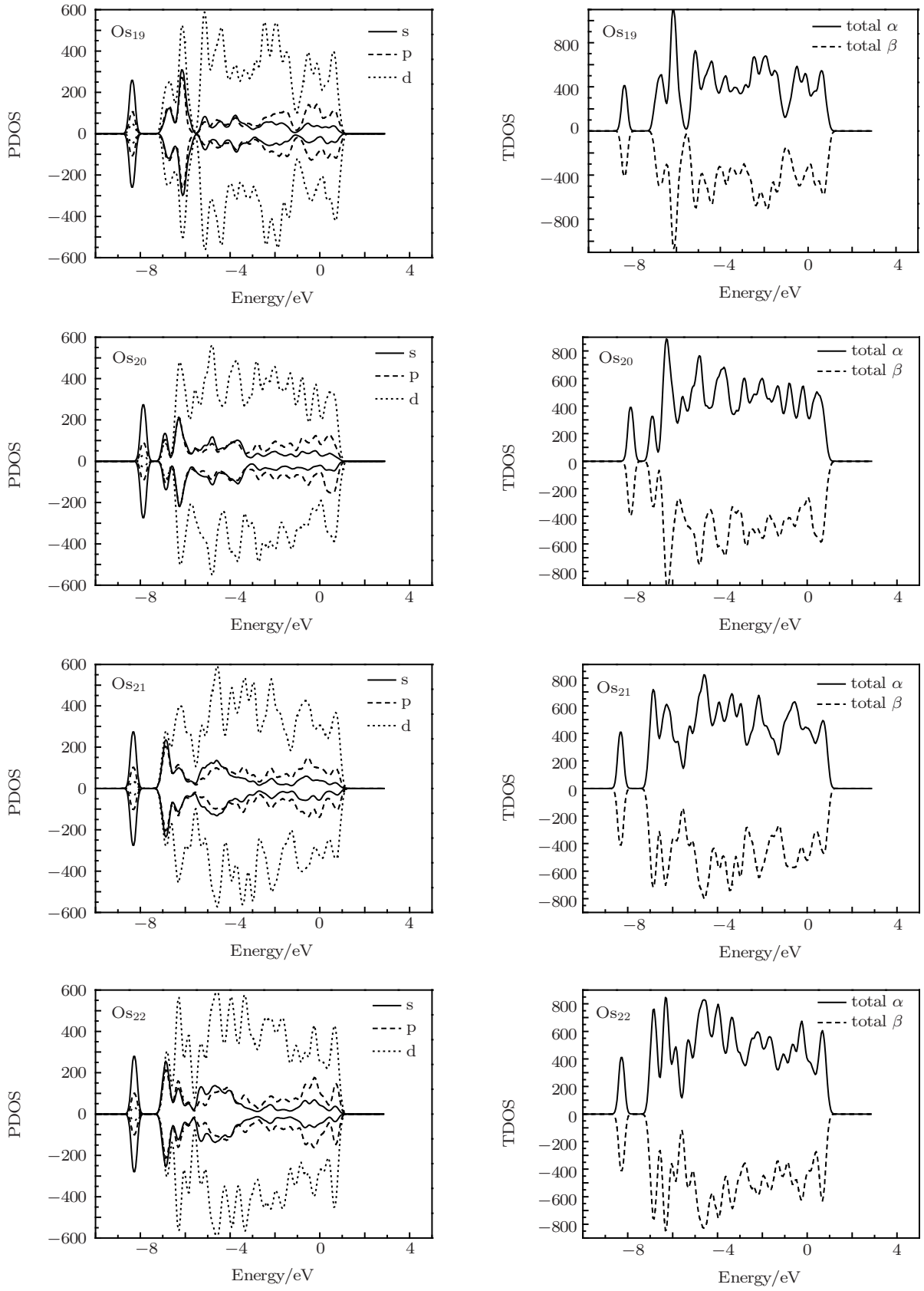

Fig. 9. Partial densities of states (PDOS) of s, p, and d orbitals and total densities of states (TDOS) of osmium clusters with $n = 19 \sim 22$. The vertical line indicates the Fermi level.

In order to describe the local magnetic moment of each atom and its contribution to the total magnetic moment, we give the electron spin density maps of four typical clusters in Fig. 11. The bigger the electron spin density of clusters, the more unpaired electrons around the atom and the bigger local magnetic moment there will be. Conversely, their contribu-

tions to the total magnetic moment will become smaller.[21–24] In Fig. 11, the cluster with an atom staying in its center (especially the close-packed hexagonal cluster with two atoms staying in its center) has the smallest spin density, almost invisible. It illustrates the electrons around these atoms are all paired, forming stable chemical bonds. When $n = 14$, the cluster has very good symmetry, in which all of the electrons around the atoms are paired, except the two atoms in the center. It means that their contributions to the total magnetic moment are almost the same. But in the Os_{20} cluster, the contributions of atoms mainly come from the cage structure in the right as shown in Fig. 11, which may be because the cage structure plays a leading role in the chemical properties when $n = 20$. This phenomenon accords with the stability analysis.

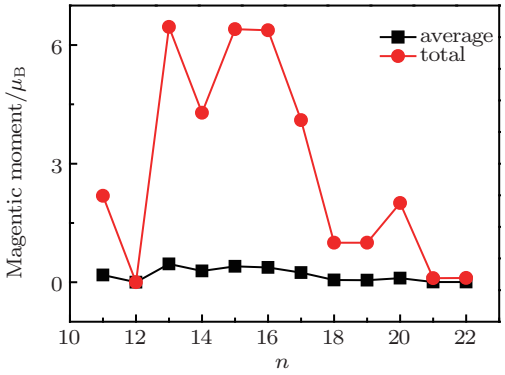

Fig. 10. (color online) Size-dependencies of average magnetic moment and total magnetic moment of Os_n clusters for the lowest-energy structure.

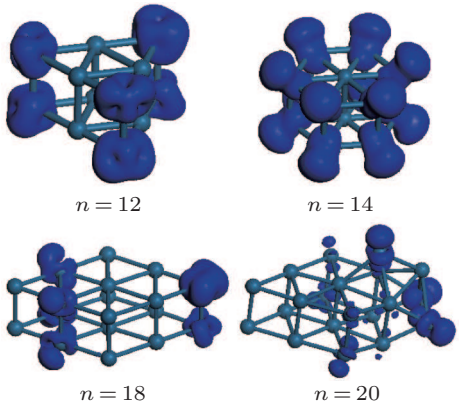

Fig. 11. (color online) Electron spin density maps of Os_n ($n = 12$, 14, 18, 20) clusters at the ground state.

4. Conclusion

Using PW91 functional within GGA, the structure and magnetic properties of Os_n ($n = 11 \sim 22$) clusters are determined. For each cluster size, an extensive search for the lowest-energy structure has been conducted by considering a number of structural isomers. The most favorite geometries of Os_n clusters with the sizes of $n = 11 \sim 18$ each turn into a cage that is somewhat compressed, most of these cages are based on the close-packed hexagonal structure, and from Os_{19} to Os_{22} cluster the ground-state seems to favor the globular cage, with Os_{19} cluster being the change point. According to the second-order energy difference and the HOMO–LUMO gaps, Os_n clusters at $n = 14$ and 18 might possess relatively high stabilities, which means that the osmium clusters possess magic numbers of $n = 14$, 18. As the partial DOS and the total DOS described, the 5d electrons play a dominant role in the chemical reaction of Os_n clusters. It is found that the magnetic moment of Os_n cluster is quenched around $n = 12$, and when $n = 18 \sim 22$ the values of all magnetic moments approximate to zero, due to the difference in electron transfer. Also, from the electron spin density maps, we know that the contribution to the total magnetic moment mainly comes from the periphery atoms when $n = 11 \sim 18$, and from Os_{19} to Os_{22} cluster, they mainly come from the cage structure.

References

[1] Duan H M and Zheng Q Q 2001 *Phys. Lett. A* **280** 333
[2] Feng J N, Huang X R and Li Z S 1997 *Chem. Phys. Lett.* **276** 334
[3] Xiao L and Wang L C 2004 *J. Phys. Chem. A* **108** 8605
[4] Wang J G, Zhao J J, Ma L, Wang B L and Wang G H 2007 *Phys. Lett. A* **367** 335
[5] Du J G, Sun X Y, Meng D Q, Zhang P C and Jiang G 2009 *J. Chem. Phys.* **131** 044313
[6] Dyall K G 2000 *J. Phys. Chem. A* **104** 4077
[7] Shafai G S, Shetty S, Krishnamurty S, Shah V and Kanhere D G 2007 *J. Chem. Phys.* **126** 014704
[8] Ding X L, Li Z Y, Yang J L, Hou J G and Zhu Q S 2004 *J. Chem. Phys.* **121** 2558
[9] Wang J L, Wang G H and Zhao J J 2003 *Phys. Rev. A* **68** 013201
[10] Phaisangittisakul N, Paiboon K, Bovornratanaraks T and Pinsook U 2012 *J. Nanopart. Res.* **14** 1020
[11] Ahrens B, Clarke L P, Feeder N, Khan M S, Li P, Martin J N and Raithby P R 2008 *Inorg. Chim. Acta* **361** 3117
[12] Jackson S D and Walls P B 1986 *Platin. Met. Rev.* **30** 14
[13] Zhang M, Wang M, Cui T, Ma Y M, Niu Y L and Zou G T 2008 *J. Phys. Chem. Solids* **69** 2096
[14] Yang J W, Chen X R, Luo F and Li G F 2009 *Physica B* **404** 3608
[15] Ji Z W, Hu C H, Wang D H, Zhong Y, Yang J, Zhang W Q and Zhou H Y 2012 *Acta Mater.* **60** 4208
[16] Zhang X R, Cui Y N, Hong L L and Zhang W 2009 *J. Mol. Sci.* **25** 109 (in Chinese)
[17] Zhang X R and Zhang W 2009 *Journal of Jiangsu University of Science and Technology* (Natural Science Edition) **23** 183 (in Chinese)
[18] Zhang X R, Wu L Q and Rao Q 2011 *Acta Phys. Sin.* **60** 083601 (in Chinese)
[19] Zhang X R, Wu L Q, Kang Z L and Tang H S 2011 *Acta Phys. Sin.* **60** 053601 (in Chinese)
[20] Wu Z J, Han B, Dai Z W and Jin P C 2005 *Chem. Phys. Lett.* **403** 367
[21] Chen D D, Kuang X Y, Zhao Y R, Shao P and Li Y F 2011 *Chin. Phys. B* **20** 063601
[22] Li J, Liu X Y, Zhu Z H and Sheng Y 2012 *Chin. Phys. B* **21** 033101
[23] Gu J B, Yang X D, Wang H Q and Li H F 2012 *Chin. Phys. B* **21** 043102
[24] Zhang X R, Yang X and Ding X L 2012 *Chin. Phys. B* **21** 093601